

DEPENDENCE OF THE OPTICAL/UV VARIABILITY ON THE EMISSION LINE PROPERTIES AND EDDINGTON RATIO IN ACTIVE GALACTIC NUCLEI

Y. L. AI^{1,2,3}, W. YUAN^{1,2}, H. Y. ZHOU^{4,5}, T. G. WANG^{4,5}, X.-B. DONG^{4,5}, J. G. WANG^{1,2,3}, H. L. LU^{4,5}

accepted for publication in ApJ Letter

ABSTRACT

The dependence of the long-term optical/UV variability on the spectral and the fundamental physical parameters for radio-quiet active galactic nuclei (AGNs) is investigated. The multi-epoch repeated photometric scanning data in the Stripe-82 region of the Sloan Digital Sky Survey (SDSS) are exploited for two comparative AGN samples (mostly quasars) selected therein, a broad-line Seyfert 1 (BLS1) type sample and a narrow-line Seyfert 1 (NLS1) type AGN sample within redshifts 0.3–0.8. Their spectral parameters are derived from the SDSS spectroscopic data. It is found that on rest-frame timescales of several years the NLS1-type AGNs show systematically smaller variability compared to the BLS1-type. In fact, the variability amplitude is found to correlate, though only moderately, with the Eigenvector 1 parameters, i.e., the smaller the $H\beta$ linewidth, the weaker the [O III] and the stronger the Fe II emission, the smaller the variability amplitude is. Moreover, an interesting inverse correlation is found between the variability and the Eddington ratio, which is perhaps more fundamental. The previously known dependence of the variability on luminosity is not significant, and that on black hole mass—as claimed in recent papers and also present in our data—fades out when controlling for the Eddington ratio in the correlation analysis, though these may be partly due to the limited ranges of luminosity and black hole mass of our samples. Our result strongly supports that an accretion disk is likely to play a major role in producing the optical/UV variability.

Subject headings: galaxies: active — galaxies: Seyfert — quasars: general — techniques: photometric

1. INTRODUCTION

Variation of optical/UV emission on timescales from hours to years is one of the defining characteristics of Active Galactic Nuclei (AGNs). Numerous previous studies of AGN/quasar ensembles have shown that the variability amplitude is dependent on wavelength (e.g., Cutri et al. 1985; di Clemente et al. 1996; Helfand et al. 2001), luminosity (e.g., Hook et al. 1994; Givon et al. 1999; Hawkins 2000), time lag (e.g., de Vries et al. 2005) and redshift (e.g., Vanden Berk et al. 2004), and yet has a large scatter. While it is generally believed that the optical/UV light is emitted from an optically thick accretion disk powered by a central massive black hole, the physical processes that produce its variability as observed are not understood yet. Interestingly, recent progresses link the variability with some fundamental parameters of AGN. A correlation of variability with M_{BH} was reported by Wold et al. (2007). Moreover, Wilhite et al. (2008) found correlations of the variability with both luminosity (inversely) and M_{BH} , based on which the authors speculated that variability is inversely related to the Eddington ratio ($L_{\text{bol}}/L_{\text{Edd}}$).

Prominent line emission in the optical/UV band is another defining feature of AGNs. A set of strong correlations has been revealed to link the emission line properties, i.e. a narrow $H\beta$ line associated with strong optical Fe II, weak [O III] (Boroson & Green 1992). These correlations form the so-called eigenvector 1 (E 1) of AGN, which is sugges-

tively driven by some underlying, more fundamental physical parameters, most likely the Eddington ratio (Sulentic et al. 2000; Boroson 2002; Dong et al. 2009).

However, the relationship between the above two AGN characteristics—the optical/UV variability and the emission line properties (or E1)—is poorly explored observationally so far. The same is true for the relation between the variability and the Eddington ratio. In this Letter, we report our investigation on this issue, as the first result of our comprehensive studies of AGN variability by making use of the valuable multi-epoch repeated photometric scanning of the Stripe-82 region in the Sloan Digital Sky Survey (SDSS). One virtue of our study improving upon previous ones is the inclusion of AGNs with optical spectra characteristic of narrow-line Seyfert 1 (NLS1), in addition to typical broad-line AGNs (BLAGN) of the broad-line Seyfert 1 (BLS1) type, whose variability has been extensively studied. The NLS1-type AGNs extend to the extremes in the E1 space and to high $L_{\text{bol}}/L_{\text{Edd}}$ values. We use the Λ -dominated cosmology with $H_0 = 70 \text{ km s}^{-1} \text{ Mpc}^{-1}$, $\Omega_m = 0.3$, and $\Omega_\Lambda = 0.7$.

2. SAMPLES AND DATA ANALYSIS

Our comprehensive study of AGN optical/UV variability (Ai et al. 2010) is carried out based on two comparative BLAGN samples, a BLS1-type sample and a NLS1-type sample, selected from the SDSS Data Release 3 in the Stripe-82 region. The procedure of optical spectral analysis for selecting BLAGNs has been described in detail in our previous papers (Zhou et al. 2006; Dong et al. 2008), and the NLS1-type sample is taken from Zhou et al. (2006). The sample selection and photometric data analysis, including photometric calibration and measurement of variability, are described in detail in Ai et al. (2010), and is only briefly summarized here.

The sample selection criteria are: (a) located within the Stripe-82 region ($RA > 310^\circ$ or $< 59^\circ$ and $-1.25^\circ < Dec < 1.25^\circ$); (b) redshift $z < 0.8$ ($H\beta$ present in spectra) and the

ayl@ynao.ac.cn, wmy@ynao.ac.cn

¹ National Astronomical Observatories/Yunnan Observatory, Chinese Academy of Sciences, Kunming, Yunnan, P.O. BOX 110, P.R.China

² Key Laboratory for the Structure and Evolution of Celestial Objects, Chinese Academy of Sciences

³ Graduate School of the Chinese Academy of Sciences, 19A Yuquan Road, P.O. Box 3908, Beijing 100039, China

⁴ Center for Astrophysics, University of Science and Technology of China, Hefei, Anhui, 230026, P.R.China

⁵ Joint Institute of Galaxies and Cosmology, SHAO and USTC

broad component of $H\beta$ or $H\alpha$ detected at $> 10\sigma$; (c) classified as ‘star’ in *all* of the five bands by the SDSS photometric pipeline so as to eliminate the contamination from host galaxy starlight; (d) non-radio-loud, so as to eliminate possible contamination from jet emission (Yuan et al. 2008); (e) a BLS1- and NLS1-type dividing line as the broad $H\alpha/H\beta$ FWHM $= 2,200 \text{ km s}^{-1}$, following Zhou et al. (2006, see also Gelbord et al. 2009). All of our NLS1-type objects also meet the conventional $[\text{O III}]/H\beta < 3$ criterion for NLS1s (see Zhou et al. 2006, for details).

The above selections result in 58 NLS1-type and 217 BLS1-type AGNs. Furthermore, since we aim at a comparative study of the BLS1- and NLS1-type, we require the two samples to have statistically compatible distributions on the redshift–luminosity ($z-M_i$) plane. As the BLS1-type AGNs largely outnumber the NLS1-type ones, a subsample of the former is then extracted to mimic the $z-M_i$ distribution of the latter. We try to retain the NLS1-type sample (with only a few outliers discarded), and prune the BLS1 sample by randomly selecting its objects falling within sub-regions divided on the $z-M_i$ plane, with a BLS1/NLS1 ratio consistent with 2:1. This results in two final working samples, 55 NLS1- and 108 BLS1-type AGNs, which are statistically compatible on the redshift–luminosity plane [Figure 1; the 2-D Kolmogorov-Smirnov test (Press et al. 1992) yields a chance probability of 0.43 that they have the same $z-M_i$ distributions].

The two working samples consist of mostly quasars with $M_i < -23 \text{ mag}$ and $z \simeq 0.3-0.8$. They can be considered as optically and homogeneously selected, with reliably measured continuum and emission line parameters (see Zhou et al. 2006; Dong et al. 2008). Their physical parameters span almost the whole range of BLAGNs with $\text{FWHM}(H\beta) \simeq 1000-8000 \text{ km s}^{-1}$, black hole mass $M_{\text{BH}} = 10^{6.5} - 10^9 M_\odot$, luminosity (i -band) $M_i = -22 \sim -26$, and the Eddington ratio $L_{\text{bol}}/L_{\text{Edd}} = 0.01-1$.

The Stripe-82 region was repeatedly scanned during the SDSS-I phase (2000-2005) under generally photometric conditions and the data were well calibrated (Lupton et al. 2002). This region was also scanned repeatedly over the course of three 3-month campaigns in successive three years in 2005–2007 known as the SDSS Supernova Survey (SN survey). In this work we use the photometric data obtained during the SDSS-I phase from Data Release 5 (DR5, Adelman-McCarthy et al. 2007) and the SN survey during 2005. We use the PSF magnitudes.

Observations in the SN survey were sometimes performed in non-photometric conditions. At the time when this work was started only the un-calibrated source catalogs were available. Thus we need to calibrate out possible photometric ‘zero-point’ offsets in the SN data against the DR5 magnitudes, using stars in the same fields as ‘standards’. The photometric calibration is performed field-by-field for each of the SN survey fields (100 arcmin^2 patches) in which our sample objects locate. ‘Standard stars’ with good measurements (high quality photometry) are selected following the recommendations of the SDSS instructions⁶. The differential magnitudes of the calibrating stars (50–200 in numbers) between the SN survey and DR5 observations ($\Delta m = m_{\text{SN}} - m_{\text{DR5}}$) are calculated, and their weighted mean is set to zero, $\langle \Delta m \rangle = 0$. In this way the zero-point offsets of the SN survey photometry are determined, which have (systematic) uncertainties

$< 0.01 \text{ mag}$ relative to the reference DR5 data for all the fields. The total systematic errors of the calibrated SN survey photometry are thus the quadratic sum of the above item and those of the DR5 photometry (Ivezić, et al. 2004). The overall (systematic and statistical) photometric errors of the calibrated SN survey magnitudes have a median of $\approx 0.03 \text{ mag}$ for the g , r , and i bands, and $\approx 0.04 \text{ mag}$ for the u and z bands, which are comparable to those in the DR5 data. The reliability of our photometric calibration can be demonstrated by examining the calibrated SN survey data of the 14 Landolt photometric standard stars (Landolt 1992) locating in Stripe-82; none of them is found to show detectable variability.

For each of the objects there are typically ~ 27 observations (14 from the SN survey during 2005) spanning ~ 5 years (see Figure 2 for an example lightcurve). The optical variability is commonly measured by the variance of observed magnitudes, with the contribution due to measurement errors subtracted; the intrinsic amplitude σ_m is given by the square root of this variance (e.g. Vanden Berk et al. 2004; Sesar et al. 2007). We adopt a formalism similar to that used in Sesar et al. (2007),

$$\Sigma = \sqrt{\frac{1}{n-1} \sum_{i=1}^N (m_i - \langle m \rangle)^2}, \quad (1)$$

where $\langle m \rangle$ is the weighted mean, and

$$\sigma_m = \begin{cases} (\Sigma^2 - \xi^2)^{1/2}, & \text{if } \Sigma > \xi, \\ 0, & \text{otherwise.} \end{cases} \quad (2)$$

Here the contribution to the variance due to measurement errors ξ is estimated directly from the errors of observed individual magnitudes ξ_i (including both the statistical and systematic errors), as

$$\xi^2 = \frac{1}{N} \sum_{i=1}^N \xi_i^2, \quad (3)$$

rather than that in Sesar et al. (2007) where a fitted error relation from a large sample was used. Such an estimation of ξ was also used in Rodriguez-Pascual et al. (1997), though in the flux rather than magnitude domain.

We approximate the derived amplitude σ_m for a filter band as that at its effective wavelength λ_0 . For an object of redshift z , λ_0 corresponds to a wavelength $\lambda = \lambda_0/(1+z)$ in the object’s rest frame. Thus for each object the variability σ_m at five rest wavelengths are sampled which correspond to the five SDSS bands.

3. RESULTS

We find that the long-term variability with amplitudes σ_m greater than $\approx 0.05 \text{ mag}$ (approximately the minimum amplitude detectable in this work) is ubiquitous in our AGNs. The previously known strong dependence of the amplitude on (rest-frame) wavelength is also detected. To eliminate this effect in the following analysis, we divide the whole rest wavelength range sampled here, $1900-7100 \text{ \AA}$, into five bins of equal bin-size in $\log \lambda$ (see Table 1), and treat the variability in each bin separately. In a few objects where more than one measurement falling into one wavelength bin, the averaged σ_m values is used for that bin. We find that, although the wavelength dependence is negligible within a wavelength bin, large scatters of variability clearly remain (see Figure 3). Of particular interest, we find that NLS1-type AGNs have systematically lower variability than BLS1-type AGNs in all the

⁶ <http://www.sdss.org/dr7/products/catalogs/flags.html>

five wavelength bins, which are moderately significant (using the Student's t -test for the sample means yields probability levels of 0.001–0.01). A question is: what causes the large diversity of the variability, or what controls the variability amplitude? It is well known that large scatters in some of the AGN observables can be reduced when the set of Eigenvector 1 correlations are considered, in which AGNs lie continuously with NLS1-type clustering at one end. Below we extend these correlations to including variability amplitude.

3.1. Correlations with the E1 parameters

Correlations are tested between the variability amplitude σ_m and several well known E1 parameters, namely, $H\beta$ FWHM, the relative strength of the [O III] and Fe II emission lines. The latter two are measured by the intensity ratios to $H\beta$, i.e. $R_{5007} \equiv [\text{O III}]\lambda 5007/H\beta$ (where the total flux of $H\beta$ is used) and $R_{4570} \equiv \text{Fe II}\lambda\lambda 4434 - 4684/H\beta^b$ (where Fe II $\lambda\lambda 4434 - 4684$ denotes the Fe II multiplets flux integrated over 4434–4684 Å, and $H\beta^b$ the flux of the broad component of $H\beta$). The non-parametric Spearman rank statistic is used. The correlations are tested for the combined BLS1- and NLS1-type AGN sample as well as for each sample separately. The results are summarized in Table 1, with the Spearman's coefficient r_s and the two-tailed probability for the null hypothesis of no correlation. Figure 3 shows the data in *one* of the wavelength bins as examples.

For the combined AGN sample in all the wavelength bins, there exist moderate yet interesting correlations between the variability and the three E1 parameters, which are statistically significant. The smaller the $H\beta$ linewidth is, the weaker the [O III] and the stronger the Fe II emission, and the smaller the variability amplitude. Among them, the strongest correlations are those with the Fe II strength R_{4570} ($r_s \sim -0.4$), followed by those with FWHM($H\beta$), while those with R_{5007} are the weakest. Some of the correlations still remain significant even when the two samples are considered separately.

It is thus clear that the large scatter in the optical/UV variability as observed can, at least to some extent, be attributed to the distribution of AGN across the E1 parameter space. Our finding of the lower ensemble variability of NLS1- compared to BLS1-type AGNs is just a manifestation of these correlations, for the former have smaller linewidths by definition and generally weaker [O III] and stronger Fe II emission than the latter. Given such significant and interesting correlations, we suggest that the E1 correlations may be extended to those involving the variability in the optical/UV band.

3.2. Link with the Eddington ratio, luminosity and black hole mass

There have been suggestions that the underlying driver of the E1 correlations is most likely the Eddington ratio (Boroson & Green 1992; Sulentic et al. 2000; Boroson 2002). Here we test the dependence of the variability on $L_{\text{bol}}/L_{\text{Edd}}$ explicitly. We also examine the variability dependence on luminosity and M_{BH} , as claimed in previous studies. M_{BH} are estimated using the scaling relation given in Greene & Ho (2005) from the broad $H\beta$ FWHM and the 5100 Å luminosity (L_{5100}), which are taken from or measured in the same way as in Zhou et al. (2006). To calculate $L_{\text{bol}}/L_{\text{Edd}}$ the bolometric luminosities are estimated as $L_{\text{bol}} = 9L_{5100}$ (Elvis et al. 1994). The results of the correlation tests are listed in Table 1, and the data in the 2500–3300 Å bin are demonstrated in Figure 4 as an example.

Of particular interest, the strongest correlation is an inverse correlation of the variability with $L_{\text{bol}}/L_{\text{Edd}}$ ($r_s \sim -0.4$), which is the case for all the wavelength bins. The correlation is present in not only the combined BLS1- and NLS1-type AGN sample but also the individual samples separately, although it is only marginal in the NLS1-type sample alone (possibly due to its narrow $L_{\text{bol}}/L_{\text{Edd}}$ range). These correlations are as strong as the above σ_m – R_{4570} correlation. In addition, the combined two samples also show a positive correlation between the variability and black hole mass, though it is considerably weaker compared to that with $L_{\text{bol}}/L_{\text{Edd}}$. For luminosity (L_{5100} used here), however, there is essentially no significant correlation found in all the wavelength bins except 2500–3300 Å, in which a weak inverse correlation may be marginally present ($P \sim 0.01$).

Since $L_{\text{bol}}/L_{\text{Edd}}$ appears to correlate with M_{BH} in our samples (as commonly found in optically selected AGN samples with a limited luminosity range), one or both of their correlations with the variability may not be as significant as it appears to be, or one may even be spurious and induced from the other. We try to eliminate this possible effect of the third variant using the partial Spearman correlation test (see the last two columns in Table 1 for results). We first re-examine the correlation between σ_m and M_{BH} by taking into account their respective correlations with $L_{\text{bol}}/L_{\text{Edd}}$. It turns out that, in all the wavelength bins, the correlations with M_{BH} vanish when the dependence on $L_{\text{bol}}/L_{\text{Edd}}$ is taken into account. However, the same treatment for the σ_m – $L_{\text{bol}}/L_{\text{Edd}}$ relation, with the effect of M_{BH} eliminated, still yields significant, though somewhat reduced, inverse correlations in three wavelength bins. We thus conclude that the σ_m – $L_{\text{bol}}/L_{\text{Edd}}$ correlation is genuine, regardless of the σ_m – M_{BH} correlation. The latter, as apparently seen in the data and previously reported (Wold et al. 2007; Wilhite et al. 2008), is consistent with being induced from the former.

4. DISCUSSION AND CONCLUSIONS

It is intriguing that the optical/UV variability is closely related to the AGN E1 parameters. This can be understood in light of the same interesting correlations with the Eddington ratio, also found here, provided that $L_{\text{bol}}/L_{\text{Edd}}$ is indeed the underlying driver of the E1 correlations. Since the variability– $L_{\text{bol}}/L_{\text{Edd}}$ correlation is significant enough for the BLS1-type sample alone without including NLS1-type, our result does not rely on the M_{BH} (thus $L_{\text{bol}}/L_{\text{Edd}}$) estimation for NLS1-type AGNs, which is still somewhat controversial. The fact that the correlations of the variability with the E1 parameters and $L_{\text{bol}}/L_{\text{Edd}}$ are as strong as those among the E1 parameters and $L_{\text{bol}}/L_{\text{Edd}}$ themselves suggests that the E1 correlations may be extended to those involving the optical/UV variability.

The correlation between the variability and M_{BH} , though also present in our data, turns out to be insignificant when $L_{\text{bol}}/L_{\text{Edd}}$ is taken into account. We thus suggest that such a correlation, as claimed in recent studies (Wold et al. 2007; Wilhite et al. 2008), might be spurious and induced from the variability– $L_{\text{bol}}/L_{\text{Edd}}$ relation. The previously known variability–luminosity inverse correlation is found to be insignificant or at most weak in our data. This may be partly due to the fact that our analysis is capable of recovering AGNs (some are NLS1-type) with small variability in the low luminosity regime (see Figure 4) which were largely missed in previous work for various reasons. However, our morphology and redshift cuts restrict both the luminosity and M_{BH} ranges of our samples, which are important for comparisons

with previous work. For example, Vanden Berk et al. (2004) have shown that a factor of 100 change in luminosity corresponds to a factor of 4 change in variability. Thus it cannot be ruled out that the lack of significant dependence on either luminosity or M_{BH} may be due to their limited ranges in our samples.

The ensemble weaker variability of NLS1- compared to BLS1-type AGNs, as evidently found here and also suggested by Klimek et al. (2004) based on a small sample, is simply a natural consequence of the correlations with the E1 parameters and the Eddington ratio. The dependence on $L_{\text{bol}}/L_{\text{Edd}}$ can be understood qualitatively in terms of decreasing variability with increasing radius of the accretion disk, independent of the actual physical processes that drives the variability. Such radius-dependent variability is suggested by the fact that the variability amplitude increases as wavelength decreases (e.g. Vanden Berk et al. 2004) in the context of thermal disk model. As the accretion rate \dot{m} (in units of the Eddington rate) increases, the continuum emission region that dominates a given waveband moves outward to a larger radius r (in units of the Schwarzschild radius) because of $\lambda \propto T^{-1} \propto (M/\dot{m})^{1/4} r^{3/4}$; and hence decreasing variability is expected. We note that such a trend of optical variability seems at odds with that in the X-ray band (Papadakis 2004), though in the X-ray case more convincing results are needed. The different behavior may result from the different mechanisms and emitting regions of the radiation, as well as different variability mechanisms, in the two bands (see e.g. Uttley 2006).

Our finding of the strong correlations of the variability with the E1 parameters and $L_{\text{bol}}/L_{\text{Edd}}$ imposes interesting constraints to AGN variability models. Foremost, this indicates that the optical/UV variability must be intrinsic to AGN ac-

tivity; any external scenarios, such as gravitational microlensing (Hawkins 2000), multiple supernovae and star collisions (Cid Fernandes et al. 2000), can be ruled out as the dominant process. For intrinsic variability models, it is not clear whether the mechanism causing variability is some minor, secondary effect or related to the main energy generation process, as discussed in Gaskell (2008). Our result favors the latter since the Eddington ratio is directly related to the mass accretion rate of AGN at a given accretion efficiency. The correlation with $L_{\text{bol}}/L_{\text{Edd}}$ as found here suggests that the accretion disk most likely plays a critical role in producing the observed optical/UV variability, since the disk structure is depending on the mass accretion rate. For instance, the model proposed by Li & Cao (2008) that the variability is caused by change of accretion rates can reproduce *qualitatively* the observed inverse variability- $L_{\text{bol}}/L_{\text{Edd}}$ relation (Li S., private communication).

We thank the referees for helpful comments and suggestions. W.Y. thanks S. Li and B. Czerny for useful discussions. This work is supported by Chinese NSF grants NSF-10533050, the National Basic Research Program of (973 Program 2009CB824800, 2007CB815405). Funding for the SDSS and SDSS-II was provided by the Alfred P. Sloan Foundation, the Participating Institutions, the National Science Foundation, the U.S. Department of Energy, the National Aeronautics and Space Administration, the Japanese Monbukagakusho, the Max Planck Society, and the Higher Education Funding Council for England. The SDSS Web Site is <http://www.sdss.org/>.

REFERENCES

- Adelman-McCarthy, J. K., et al. 2007, *ApJS*, 172, 634
 Ai, Y. L., Yuan, W., Zhou, H.-Y. 2010, in prep.
 Boroson, T. A., & Green, R. F. 1992, *ApJS*, 80, 109
 Boroson, T. A. 2002, *ApJ*, 565, 78
 Cid Fernandes, R.; Sodré, L., Jr., & Vieira da Silva, L., Jr. 2000, *ApJ*, 544, 123
 Cutri, R. M., Wisniewski, W. Z., Rieke, G. H. & Lebofsky, M. J. 1985, *ApJ*, 296, 423
 de Vries, W. H., Becker, R. H., White, R. L., & Loomis, C. 2005, *AJ*, 129, 615
 di Clemente, A., Giallongo, E., Natali, G., Trevese, D., & Vagnetti, F. 1996, *ApJ*, 463, 466
 Dong, X.-B., Wang, T.-G., Wang, J.-G., Yuan, W.-M., Zhou, H.-Y., Dai, H.-F. & Zhang, K. 2008, *MNRAS*, 383, 581
 Dong, Xiao-Bo, Wang, Ting-Gui, Wang, Jian-Guo, Fan, Xiaohui, Wang, Huiyuan, Zhou, Hongyan, & Yuan, Weimin, 2009, *ApJ*, 703, 1
 Elvis, M., et al. 1994, *ApJS*, 95, 1
 Gaskell, C. M. 2008, *RMxAC*, 32, 1
 Gelbord, J. M., Mullaney, J. R., & Ward, M. J. 2009, *MNRAS*, 397, 172
 Giveon, U., Maoz, D., Kaspi, S., Netzer, H., & Smith, P. S. 1999, *MNRAS*, 306, 637
 Greene, J. E., & Ho, L. C. 2005, *ApJ*, 630, 122
 Hawkins, M. R. S. 2000, *A&AS*, 143, 465
 Helfand, D. J., Stone, R. P. S., Willman, B., White, R. L., Becker, R. H., Price, T., Gregg, M. D., & McMahon, R. G. 2001, *AJ*, 121, 1872
 Hook, I. M., McMahon, R. G., Boyle, B. J., & Irwin, M. J. 1994, *MNRAS*, 268, 305
 Ivezić, Ž., et al. 2004, *Astron. Nachr.*, 325, 583
 Klimek, E. S., Gaskell, C. M., Hedrick, C. H. 2004, *ApJ*, 609, 69
 Landolt, Arlo U. 1992, *AJ*, 104, 340
 Li, Sh.-L., & Cao, X.-W. 2008, *MNRAS*, 387, 41
 Lupton, R. H., et al. 2002, *Proc. SPIE*, 4836, 350
 Papadakis, I. E. 2004, *MNRAS*, 348, 207
 Press, W. H., Teukolsky, S. A., Vetterling, W. T., & Flannery, B. P. 1992, *Numerical Recipes in Fortran* (2nd. ed., Cambridge: Cambridge Univ. Press), 643
 Rodriguez-Pascual, P. M. et al. 1997, *ApJS*, 110, 9
 Sesar, B., et al. 2007, *AJ*, 134, 2236
 Sulentic, J. W., Zwitter, T., Marziani, P., & Dultzin-Hacyan, D. 2000, *ApJ*, 536, 5
 Uttley, P. 2006, in *ASP Conf. Ser. 360, AGN Variability from X-Rays to Radio Waves*, ed. C. M. Gaskell, I. M. McHardy, B. M. Peterson & Sergey G. Sergeev (San Francisco:ASP), 101
 Vanden Berk, D. E., et al. 2004, *ApJ*, 601, 692
 Wilhite, B. C., Brunner, R. J., Grier, C. J., Schneider, D. P., & vanden Berk, D. E. 2008, *MNRAS*, 383, 1232
 Wold, M., Brotherton, M. S., & Shang, Zhaohui. 2007, *MNRAS*, 375, 989
 Yuan, W., Zhou, H. Y., Komossa, S., Dong, X. B., Wang, T. G., Lu, H. L., & Bai, J. M. 2008, *ApJ*, 685, 801
 Zhou, H.-Y., Wang, T.-G., Yuan, W., Lu, H.-L., Dong, X.-B., Wang, J.-X., & Lu, Y.-J. 2006, *ApJS*, 166, 128

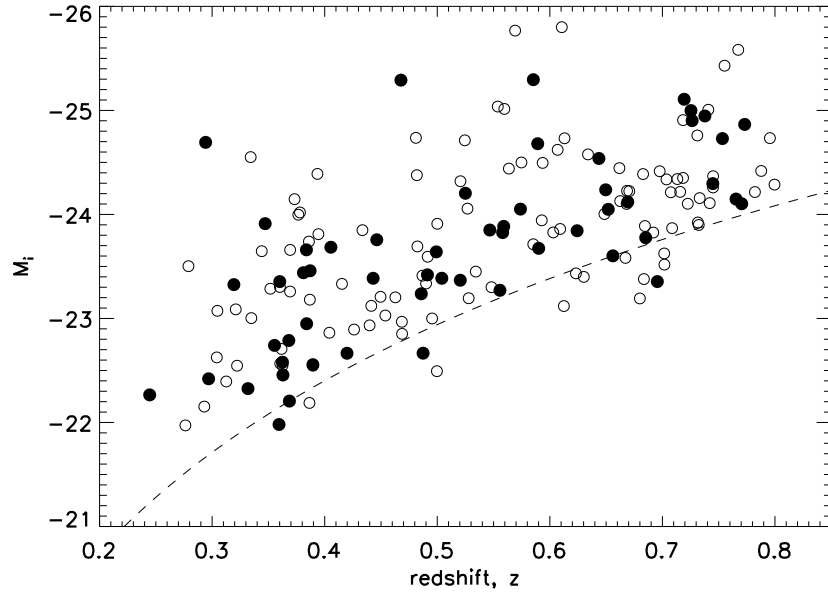


FIG. 1.— Redshift and i -band luminosity distribution of our NLS1-type AGN (filled circles) and BLS1-type (open circles) samples. The dashed curve represents the limiting magnitude for optically-selected quasars in the SDSS ($m_i = 19.1$).

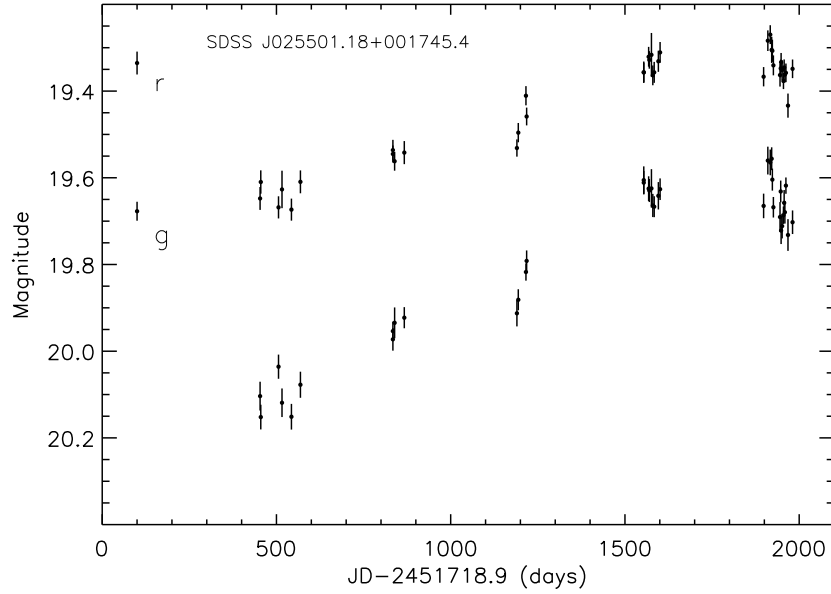


FIG. 2.— Example light curves of the NLS1-type AGN, SDSS J025501.18+001745.4, in the r and g bands.

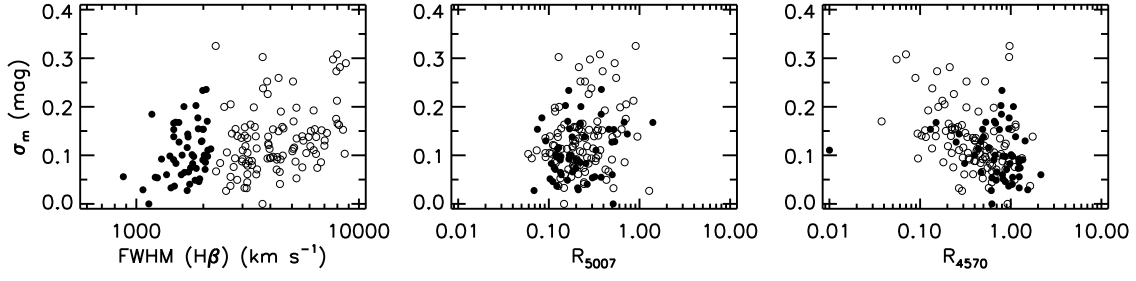


FIG. 3.— Variability amplitude versus $H\beta$ linewidth (left), the relative strength of [O III] (center) and Fe II emission (right) in *one of* the rest wavelength bins (2500–3300 Å), as an example, for BLS1-type (open) and NLS1-type AGNs (filled).

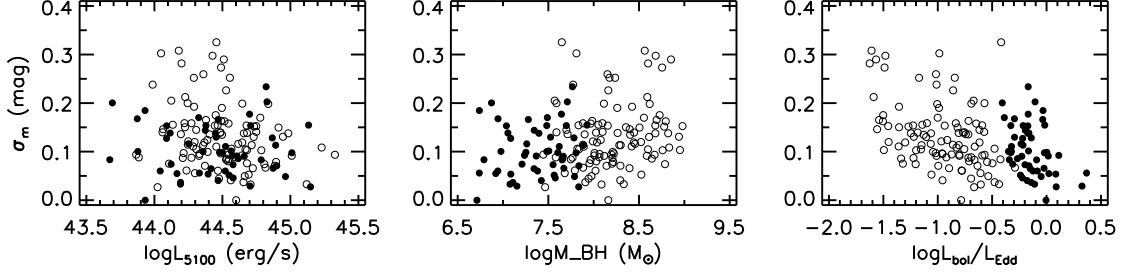


FIG. 4.— Similar to Figure 3 but for variability amplitude versus 5100 Å luminosity (left), black hole mass (center), and the Eddington ratio (right).

TABLE 1
RESULTS OF CORRELATION TESTS FOR VARIABILITY AMPLITUDE IN REST WAVELENGTH BINS: SPEARMAN CORRELATION COEFFICIENTS (AND PROBABILITY LEVELS)

Sample	^a Size	FWHM($H\beta$)	^b R_{5007}	^b R_{4570}	^b $\log(L_{5100})$	$\log(M_{BH})$	L_{bol}/L_{Edd}	^c M_{BH}	^d L_{bol}/L_{Edd}
1900 ~ 2500 Å									
all AGNs	118(0.24)	0.33(2e-04)	0.26(4e-03)	-0.39(1e-05)	-0.05(0.62)	0.32(4e-04)	-0.38(3e-05)	0.01(0.93)	-0.21(0.02)
BLS1-type	81(0.28)	0.31(5e-03)	0.30(6e-03)	-0.40(3e-04)	-0.08(0.47)	0.24(0.03)	-0.34(2e-03)	-	-
NLS1-type	37(0.41)	0.29(0.09)	0.15(0.38)	-0.26(0.12)	0.10(0.55)	0.27(0.12)	-0.21(0.22)	-	-
2500 ~ 3300 Å									
all AGNs	158(0.20)	0.32(3e-05)	0.21(7e-03)	-0.40(2e-07)	-0.16(0.04)	0.26(1e-03)	-0.38(8e-07)	-0.12(0.11)	-0.32(6e-05)
BLS1-type	104(0.25)	0.34(4e-04)	0.21(0.03)	-0.43(7e-06)	-0.25(0.01)	0.19(0.05)	-0.40(3e-05)	-	-
NLS1-type	54(0.35)	0.30(0.03)	0.18(0.18)	-0.30(0.03)	-0.08(0.57)	0.10(0.46)	-0.37(7e-03)	-	-
3300 ~ 4200 Å									
all AGNs	159(0.20)	0.31(6e-05)	0.23(3e-03)	-0.38(1e-06)	-0.13(0.09)	0.26(1e-03)	-0.37(2e-06)	-0.09(0.22)	-0.29(3e-04)
BLS1-type	105(0.25)	0.26(7e-03)	0.26(6e-03)	-0.37(9e-05)	-0.17(0.09)	0.16(0.10)	-0.31(1e-03)	-	-
NLS1-type	54(0.35)	0.24(0.09)	0.12(0.37)	-0.27(0.05)	-0.12(0.38)	0.04(0.76)	-0.35(0.01)	-	-
4200 ~ 5500 Å									
all AGNs	163(0.20)	0.34(1e-05)	0.25(1e-03)	-0.43(1e-08)	-0.08(0.33)	0.30(1e-04)	-0.38(9e-07)	-0.04(0.62)	-0.24(2e-03)
BLS1-type	108(0.25)	0.34(3e-04)	0.25(8e-03)	-0.45(1e-06)	-0.12(0.20)	0.25(9e-03)	-0.37(8e-05)	-	-
NLS1-type	55(0.34)	0.29(0.03)	0.20(0.16)	-0.34(0.01)	-0.04(0.76)	0.14(0.31)	-0.32(0.02)	-	-
5500 ~ 7100 Å									
all AGNs	104(0.25)	0.39(5e-05)	0.29(2e-03)	-0.43(5e-06)	-0.01(0.92)	0.35(3e-04)	-0.41(2e-05)	0.003(0.97)	-0.23(0.02)
BLS1-type	66(0.31)	0.44(2e-04)	0.34(5e-03)	-0.41(8e-04)	-0.01(0.92)	0.37(2e-03)	-0.44(2e-04)	-	-
NLS1-type	38(0.41)	0.30(0.07)	0.13(0.45)	-0.33(0.05)	-0.06(0.70)	0.13(0.44)	-0.36(0.03)	-	-

NOTE. — ^asample size (and the critical value above which a correlation coefficient is found from an uncorrelated sample of the size at a <1% probability); ^b R_{5007} is the intensity ratio of [O III] $\lambda 5007$ to $H\beta$, R_{4570} the intensity ratio of the Fe II multiplets to $H\beta$, L_{5100} monochromatic luminosity at 5100 Å; ^cpartial correlation between σ_m and M_{BH} , controlling for L_{bol}/L_{Edd} ; ^dpartial correlation between σ_m and L_{bol}/L_{Edd} , controlling for M_{BH} .